EGG-1183-1728

EG&G

Energy Measurements Group

Aerial Measuring Systems

MASTER

# AN AERIAL RADIOLOGICAL SURVEY OF
# ARGONNE SITE A
## PALOS HILLS, ILLINOIS

DATE OF SURVEY: MAY 1976

JUNE 1978

## NOTICE

EG&G

EGG--1183-1728

DE91 018197

AN AERIAL RADIOLOGICAL SURVEY OF

# ARGONNE SITE A

## PALOS HILLS, ILLINOIS

DATE OF SURVEY: MAY 1976

J. E. Jobst, J. M. Houk, R. A. Mohr
Project Scientists

APPROVED FOR PUBLICATION

T. P. Stuart, Manager
Remote Sensing Sciences Department



This Document is UNCLASSIFIED

G. P. Stobie
Classification Officer

This work was performed by EG&G for the United States Department of Energy, Division of Operational and Environmental Safety, under Contract No. EY-76-C-08-1183.

## ABSTRACT

An aerial radiological survey was conducted over the original site of Argonne National Laboratory, viz. Argonne Site A, and over the associated radiological waste dump, Plot M. These areas are 5 km east of the present Laboratory. The survey was performed at an altitude of 30 m on 31 May 1976 using sodium iodide detectors mounted in a helicopter.

The 2 km$^2$ aerial survey showed gamma radiation due to naturally occurring radioisotopes in the soil and due to low level concentrations of $^{137}$Cs. Subsequent soil samples showed low levels of tritium and $^{137}$Cs near Plot M. Soil samples from Site A showed low levels of $^{137}$Cs, $^{60}$Co, and other isotopes.

This survey was authorized by the United States Department of Energy (DOE) and conducted by EG&G.

# ACKNOWLEDGMENTS

The authors wish to thank Dr. Jacob Sedlet, Argonne National Laboratory, and his staff for their assistance in planning the operation and their cooperation during the survey. The cooperation of the Board of Trustees of the Village of Lemont, Illinois, was also appreciated.

Special appreciation is given to L. J. Deal, Assistant Director for Field Operations, Division of Operational and Environmental Safety, United States Department of Energy, for his support and encouragement in this program.

# TABLE OF CONTENTS



# LIST OF ILLUSTRATIONS



# LIST OF TABLES

# 1.0 INTRODUCTION

The United States Department of Energy (DOE) operates an aerial surveillance operation called AMS (Aerial Measuring Systems).* From its inception in 1958, the program has included radiological surveys of nuclear power plants, processing plants for nuclear materials, and research laboratories. AMS aircraft have been deployed to nuclear accident sites or in searches for lost radioisotopes. They were routinely used during launch operations for Apollo, Viking, and other space vehicles which contained radioisotope thermal generators. AMS aircraft also have mapping cameras and multispectral camera arrays for aerial photography, a thermal mapper for infrared imagery, a broad array of meteorological sensors, and air sampling systems for particulate and whole gas measurements.

This system is maintained and operated for the DOE by EG&G. At the request of federal (e.g., the Nuclear Regulatory Commission) or state agencies, AMS is deployed for various aerial survey operations.

# 2.0 SITE DESCRIPTION

The survey site is a heavily wooded, 2 $km^2$ plot in Cook County, Illinois, approximately 16 km southwest of Chicago Midway Airport. Illinois State Highway 171 runs through the northwestern perimeter of the Palos Hills Forest Preserve, in which the site is located. The Forest Preserve is a triangular area bounded on the north and west by the Chicago Sanitary and Ship Canal, on the south by the Calumet Sag Channel, and on the east by Kean Road. Another portion of the Preserve (not surveyed) is just south of the Calumet Sag Channel. The closest community, located just east of the Preserve, is Palos Hills.

The survey area is the original site of Argonne National Laboratory, called Site A, and a radioactive waste disposal area just north of it, called Plot M. The present Laboratory site is 5 km west of the survey area. The latter is now owned by Cook County (Illinois) and is used largely as a recreation area. Included within the survey boundaries are Horse Collar Slough, Red Gate Woods, and Henry DeTonty Woods. Bull Frog Lake and Tomahawk Slough are excluded. The western tip of Saganashkee Slough is included. The area surveyed is roughly rectangular, 2.6 km long by 0.8 km wide.

The plot plan of the original facility is shown in Fig. 1. Figure 2 is an aerial photograph of the area taken

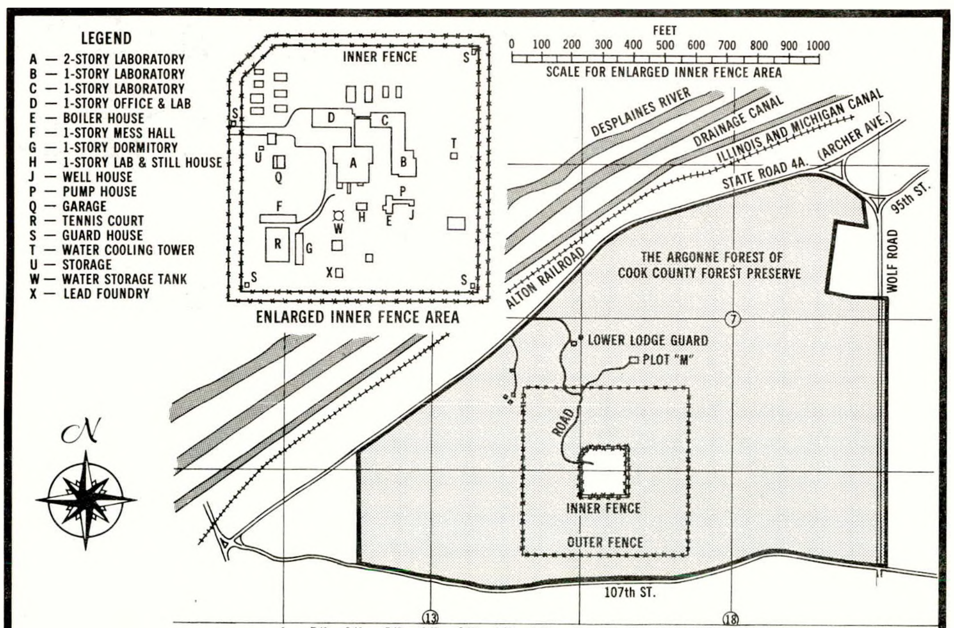


Figure 1. This drawing shows the planned location of facilities at the original Argonne Laboratory Site. All data taken from Plot Plan, Site A, Palos Park, Illinois, dated 4 October 1945, drawing No. A48.

*Formerly the Aerial Radiological Measuring System (ARMS).


Figure 2. This photograph shows Argonne Site A shortly after construction. Much of the land was covered with scrub brush or small trees, in sharp contrast to the scene today.

shortly after construction was completed. What appears as sparse vegetation and well defined ponds has now become very heavy vegetation (trees up to perhaps 20 m in height) and swampy marshes. All of the laboratory and service facilities have been razed and removed or buried, with the exception of a large metal quonset building which has nearly collapsed to the ground.

Only roads and building foundations remain of the original construction at Site A. In its center is a large stone bearing the following engraved inscription:

> "The world's first nuclear reactor was rebuilt at this site in 1943 after initial operation at the University of Chicago. This reactor (CP-2) and the first heavy-water-moderated reactor (CP-3) were major facilities around which developed the Argonne National Laboratory. This site was released by the Laboratory in 1956 and the U. S. Atomic Energy Commission then buried the reactors here."

Plot M, which is approximately 50 m by 50 m, was a radiological waste disposal area. The boundaries are clearly marked by stone corner posts. In the center of the plot is an engraved stone, split in half, which reads (in part):

> "Danger. Do not dig. Radioactive materials were buried in this area by the Metallurgical Laboratory (obliterated) Argonne National Laboratory, from (obliterated) to 1949. The burial area is outlined (obliterated) from this ...".

The remainder of the message has been destroyed by vandals.

Both Site A and Plot M are readily accessible to pedestrian traffic. Hikers and picnickers apparently use these areas quite frequently.

## 3.0 SURVEY PLAN

A highly enlarged photograph (scale: 24 m/cm) of the Palos Hills Forest Preserve was used to lay out survey lines. Twenty-eight lines, spaced 30 m apart, were laid out. Three additional lines were flown along the northwestern perimeter, roughly parallel to State Highway 171 and the Illinois Central Gulf Railroad line. All lines were flown at the nominal survey altitude of 30 m. A calibration line was flown over the Saganashkee Slough. This effectively removed all terrestrial radiation sources and allowed a background level to be established. Figure 3 shows the survey lines on an aerial photograph of the site. All aerial survey data were obtained on 31 May 1976.

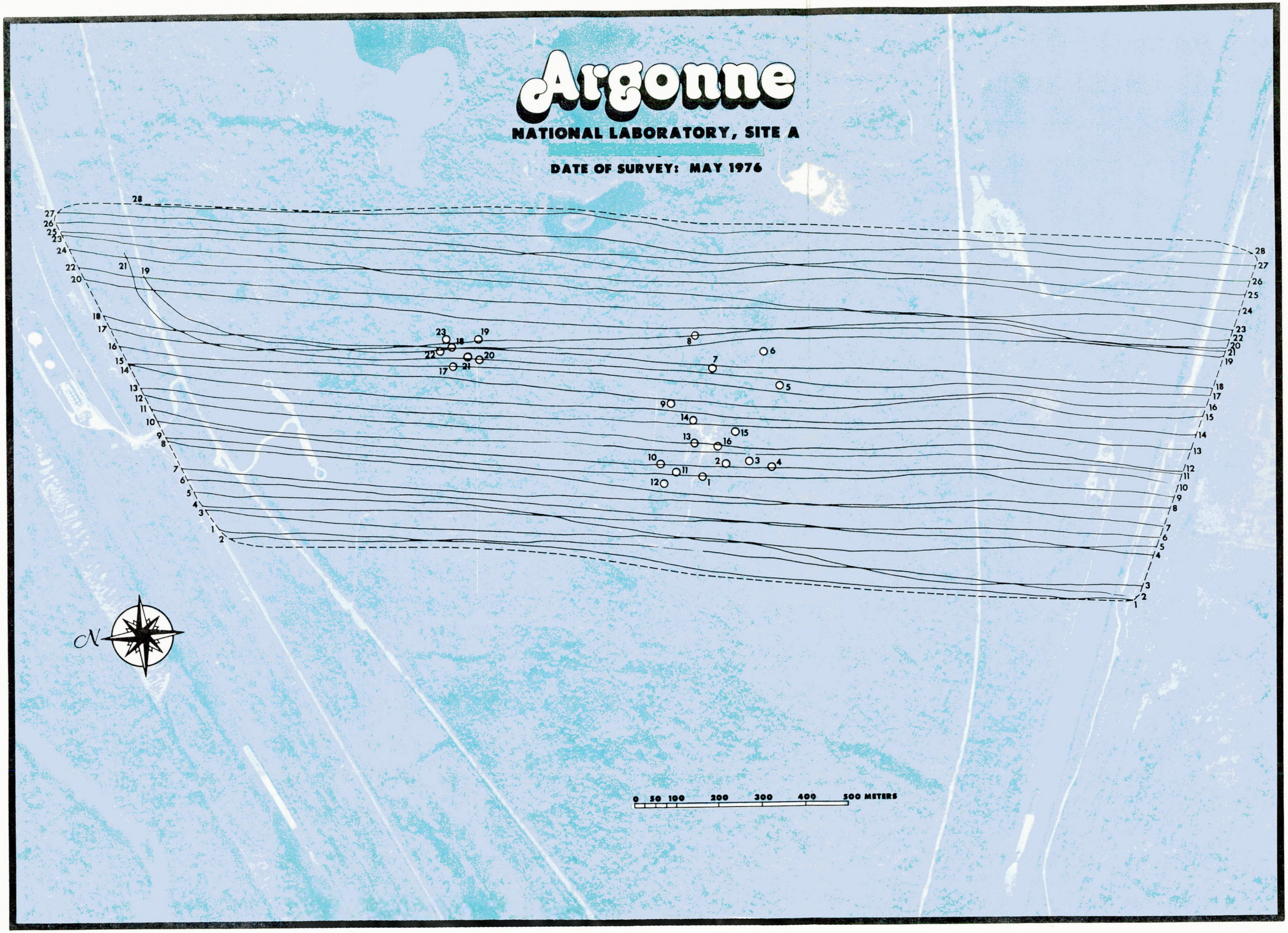


Figure 3. Twenty-eight survey lines were flown with a nominal spacing of 30 m at a survey altitude of 30 m. The actual flight paths are shown here, along with the locations of 23 soil samples at Site A and Plot M.

Twenty-three soil samples were also collected near Site A and Plot M. The locations were randomly selected. All samples were subjected to gamma ray spectrum analysis to determine isotopic composition. Samples obtained near Plot M were also analyzed for tritium concentrations. The locations of the soil samples are also shown in Fig. 3.

## 4.0 SURVEY EQUIPMENT

A Hughes H-500 helicopter, shown in Fig. 4, was used for this low altitude survey. This aircraft carried a crew of two and a light-weight version of the REDAR (Radiation and Environmental Data Acquisition and Recorder) system. Two pods, each containing ten 12.7 cm diameter by 5.1 cm thick sodium iodide NaI(Tl) detectors, were mounted on the sides of the helicopter. The preamplifier signal from each detector was calibrated with a $^{88}Y$ or $^{22}Na$ source. Normalized outputs of each detector were combined in a 10-way summing amplifier for each array. The outputs of each array were matched and combined in a 2-way summing amplifier. Finally this signal was adjusted in the analog-to-digital converter (ADC) so that the calibration peak appeared in a preselected channel of the multichannel analyzer of the REDAR.

The REDAR system contains four memories for data storage. In the first the following are stored: gross count data, single channel data, position information, live time, radar altitude, and meteorological data from various transducers. The second and third memories are operated in a flip-flop mode to store gamma ray spectral information. Memories one and, alternately,

Figure 4. The Hughes H-500 helicopter is operated by a pilot and a navigator. The latter also operates the REDAR system shown in the rear compartment. Detector pods on the left and right each contain ten sodium iodide detectors.

either two or three, are stored every three seconds on a nine track magnetic tape. The fourth memory is used solely for real time analysis on board the aircraft. Data in the fourth memory is not stored on magnetic tape.

The REDAR system can continuously acquire and record all of the following data at the indicated rates:

Table 1. REDAR System Data Input

| Parameter | Frequency |
|---|---|
| 1. 305 channel pulse-height analyzer plus live time | 3.0 sec |
| 2. 5 single channel analyzers with adjustable upper and lower discriminators | 0.2 sec |
| 3. Gross count channel (sums all counts) | 0.1 sec |
| 4. Position measurement | 1.0 sec |
| 5. Microwave Ranging System (MRS) distance measurements | 1.0 sec |
| 6. Radar altimeter | 1.0 sec |
| 7. Absolute pressure | 1.0 sec |
| 8. Outside air temperature | 1.0 sec |
| 9. Wind speed | 1.0 sec |
| 10. Wind direction | 1.0 sec |
| 11. Dew point | 1.0 sec |
| 12. True air speed | 1.0 sec |
| 13. On-top marker | As required (operator push-button) |
| 14. System configuration | 1.0 sec |
| 15. Time of day clock (HRS-MIN-SEC) | 1.0 sec |

Outputs from each detector are summed before being processed by the multichannel or single channel analyzers. Windows are set on the single channel analyzers to monitor regions of the spectrum pertinent to isotopes of interest.

All of the foregoing data inputs, including the on-top marker, may be displayed by the electronic system operator for real time monitoring. Digital data, such as count rates, meteorological information, or time of day, are displayed on one of several light emitting diode (LED) readouts. Gamma ray spectral data may be examined on the oscilloscope as the data accumulate. At any point in time a spectrum may be frozen for critical examination without affecting the continuous acquisition and recording of data. A dual pen strip chart recorder permits visual monitoring of the time variations in any two of the following: gross count, mathematical combinations of single channel windows, radar altimeter, absolute pressure, outside air temperature, dew point, or true air speed.

Data are permanently recorded on a nine track Cipher Data Products digital recorder capable of recording continuously for five hours. All data are recorded as raw information directly from sensors. The five single channels* can be set to monitor natural, cosmic, or man-made gamma-active nuclides by appropriate discriminator settings. Each single channel can be weighted, added to, or subtracted from other single channels. Appropriately weighted data can be plotted in real time on the dual strip chart recorder aboard the aircraft, with filtering times between 0.2 seconds and 16 seconds. Hence, when the operator is searching for a particular radionuclide, the single channels are set up to enhance the capability of detecting this source in real time.

The helicopter position was established with two systems: a Trisponder/202A microwave ranging system, and an AL-101 radio altimeter. The Trisponder master station, mounted in the helicopter, interrogated two remote transceivers mounted on towers outside the survey area, one on the water tower of the Village of Lemont, Illinois, the other on an Argonne National Laboratory tower. By measuring the round-trip propagation time between the master and remote stations, the master computed the distance to each. These distances were recorded on magnetic tape each second. In subsequent computer processing they were converted to position coordinates.

The radio altimeter similarly measured the time lag for the return of a pulsed signal and converted this to aircraft altitude. For altitudes up to 150 m the accuracy was ± 0.6 m or ± 2%, whichever is greater. These data were also recorded on magnetic tape so that any variations in gamma signal strength caused by altitude fluctuation could be accurately compensated.

The detectors and electronic systems which accumulate and record the data are described only briefly here. They are described in considerable detail in previous reports.[1][2]

*A misnomer. A single channel is actually a gamma energy band, defined by an upper and lower discriminator. All gamma ray counts within this energy range are counted by a "single channel".

The laboratory equipment required for the soil sample analysis included a lyophilizer system for freeze drying samples. Liquid obtained from such samples was analyzed for tritium on a Beckman LS-100 liquid scintillation system. Gamma ray analysis was performed on a low background, lithium drifted germanium detector: Ge(Li). A sodium iodide annulus detector was used in anticoincidence with the Ge(Li) detector to suppress Compton background. Gamma counts were analyzed on a 1024 channel analyzer and plotted for inspection. The equipment and techniques used for sample preparation and analysis are described in considerable detail elsewhere.[3]

## 5.0 DATA PROCESSING

Data processing was begun in the field with the REDAC (Radiation and Environmental Data Analyzer and Computer) system. This is a computer analysis laboratory, mounted in a mobile van (Fig. 5). The van and the aircraft were based at the Sugar Grove Airport near Aurora, Illinois. This site was preferable to Chicago Midway because of heavy congestion in air traffic there.

The REDAC (Fig. 6) consists primarily of two Cipher Data Products tape drives, a Data General NOVA 840 computer, two CalComp plotters, and a Tektronix CRT display screen with a hard copier. The computer has a 32 k-word core memory and an additional 1.2 x $10^6$-word disc memory. An extensive series of software routines is available for data processing.

Gamma spectral windows can be selected for any portion of the spectrum between 50 keV and 3 MeV. Weighted combinations of such windows can be

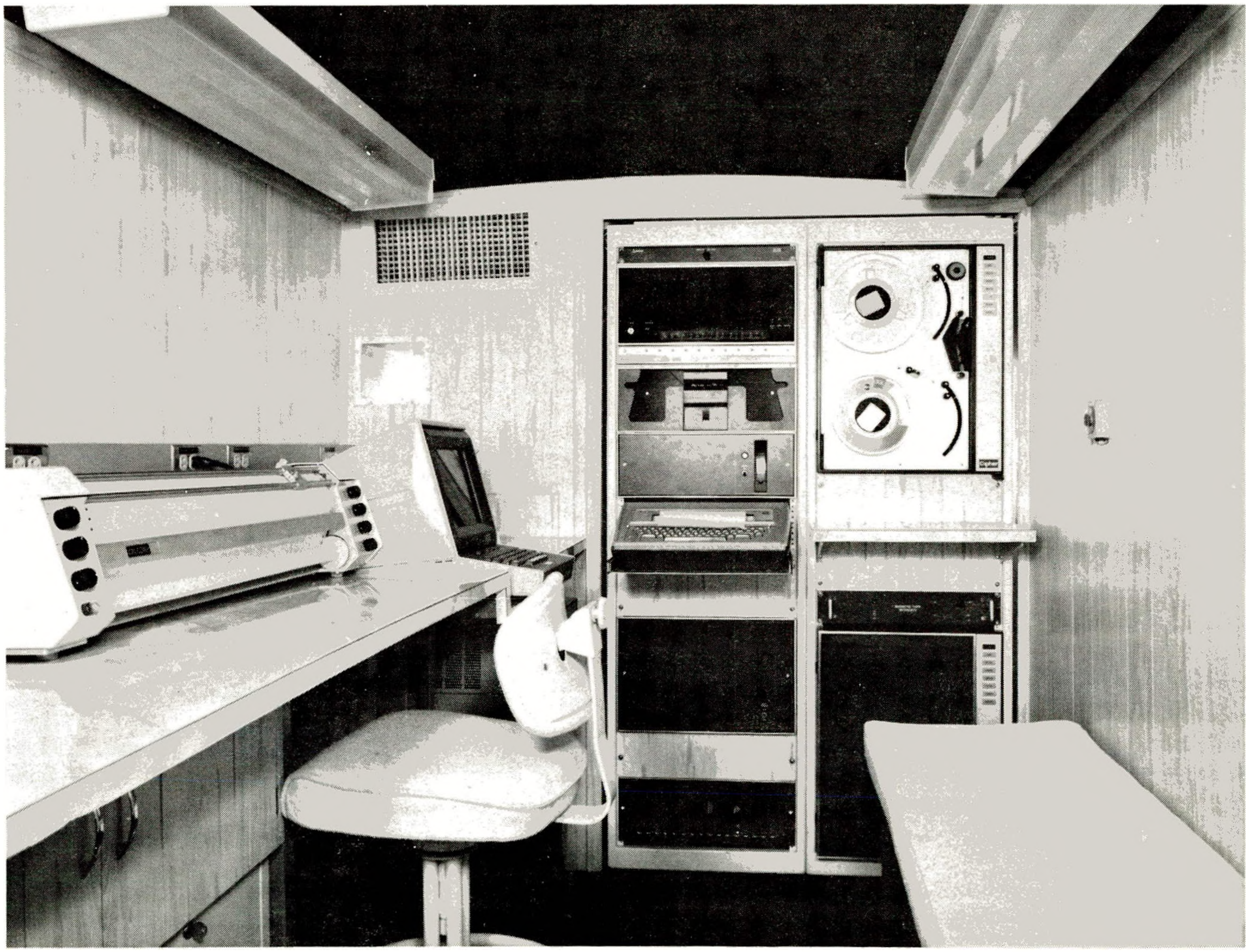

Figure 5. The heart of the REDAC system is a NOVA 840 computer. Sophisticated software routines allow preliminary isopleths to be prepared in the field. Gamma spectra may be obtained immediately after the aircraft returns from a mission.

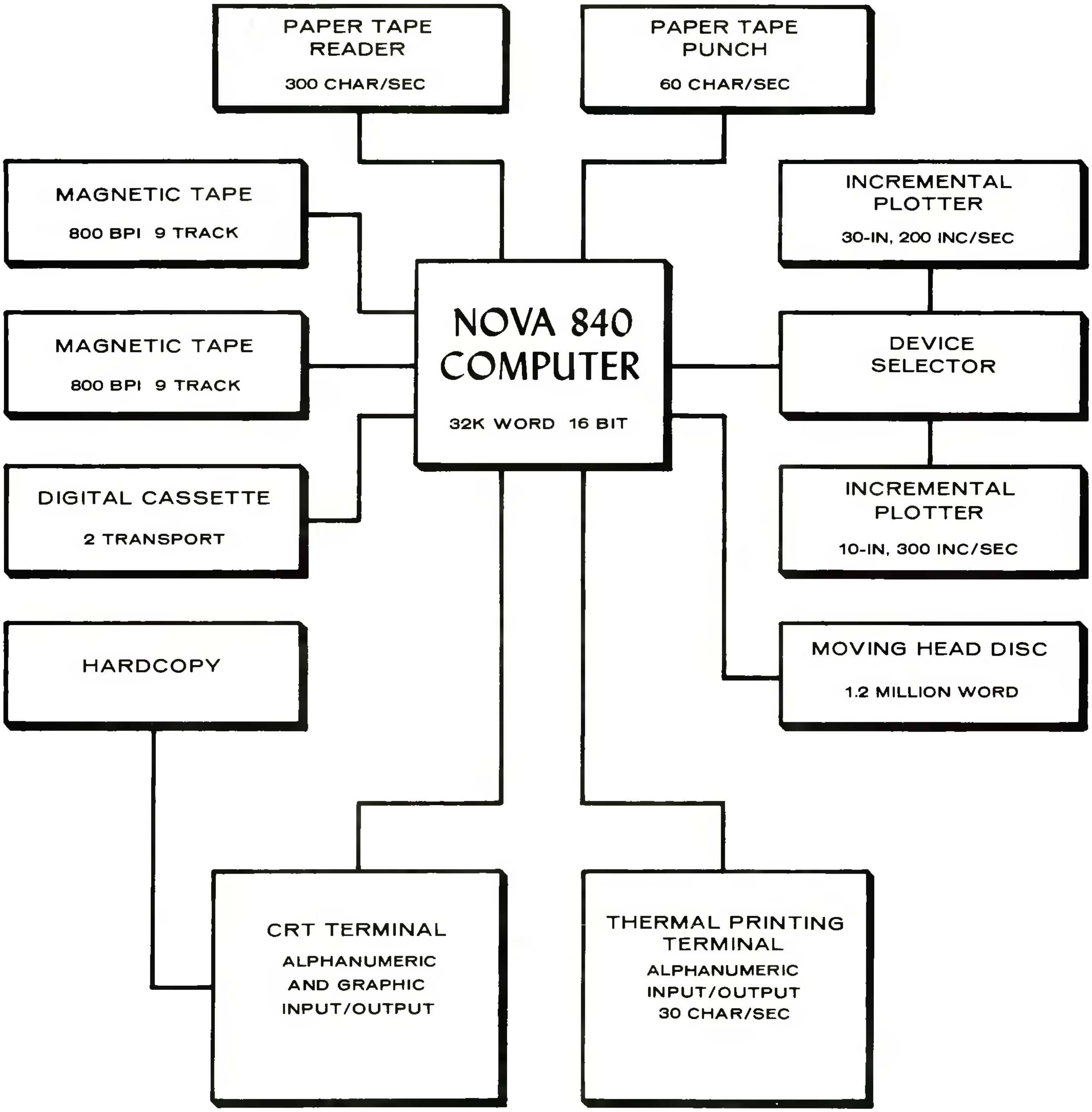


Figure 6. A block diagram of the REDAC (Radiation and Environmental Data Analyzer and Computer) system.

summed or subtracted and the result plotted as a function of time or position. By the proper selection of windows and weighting factors, it is possible to extract the photopeak count rates for radioisotopes deposited on the terrain by human activity. Such isotopes disturb the natural pattern of soil radioactivity. These photopeak count rates can then be converted to isotope concentrations or exposure rates. Spectral data can be summed over any portion of a survey flight line.

## 6.0 DATA ANALYSIS

Data analysis work has been directed to producing four specific results: (1) a gamma gross count isopleth map, (2) a $^{137}Cs$ isopleth map, (3) gamma radiation spectra from the aerial data which adequately characterize the site, and (4) soil sample isotopic analysis.

To produce a gross count isopleth, the REDAC is programmed to select gamma counts from an extremely wide energy interval (50 keV to 3.0 MeV). Gamma counts in this window are summed each second. Background from various sources is removed and an average value of the local cosmic ray exposure rate is added back in. The result is plotted as a function of position over the site. This generates a gamma gross count isopleth which characterizes the overall exposure rate at the site. Such results, which are discussed in Sec. 7.1, are readily comparable to thermoluminescent dosimeter (TLD) data or measurements of integrating gamma detectors with wide energy windows.

If gamma radiation spectra (count rate vs. energy) show photopeaks characteristic of isotopes which are not naturally occurring, special studies are made. The REDAC is programmed to select narrow windows which include the characteristic photopeaks. Computer algorithms have been devised to enhance and isolate the contribution of, say, $^{137}Cs$ or $^{60}Co$, to a normal background spectrum. Isopleths for these isotopes are then plotted for comparison with gross count spectra.

Gamma spectra from aerial data over Site A and Plot M show naturally occurring radioisotopes and apparent concentrations of $^{137}Cs$. Hence, the computer was programmed to determine the ratio of gamma counts in two windows, 0.600 to 0.740 MeV, and 0.750 to 1.000 MeV. The first contains the prominent 0.662 MeV gamma ray photopeak of $^{137}Cs$. The second contains primarily the photopeaks due to naturally occurring radioelements. Both contain scattered gammas and the Compton tails of many higher energy gammas.

The ratio between the windows is calculated for each 3-second data spectrum which corresponds to approximately 100 m of flight path. The frequency distribution of these ratios (Fig. 7) for a set of data will be normal in shape if $^{137}Cs$ is either absent, randomly

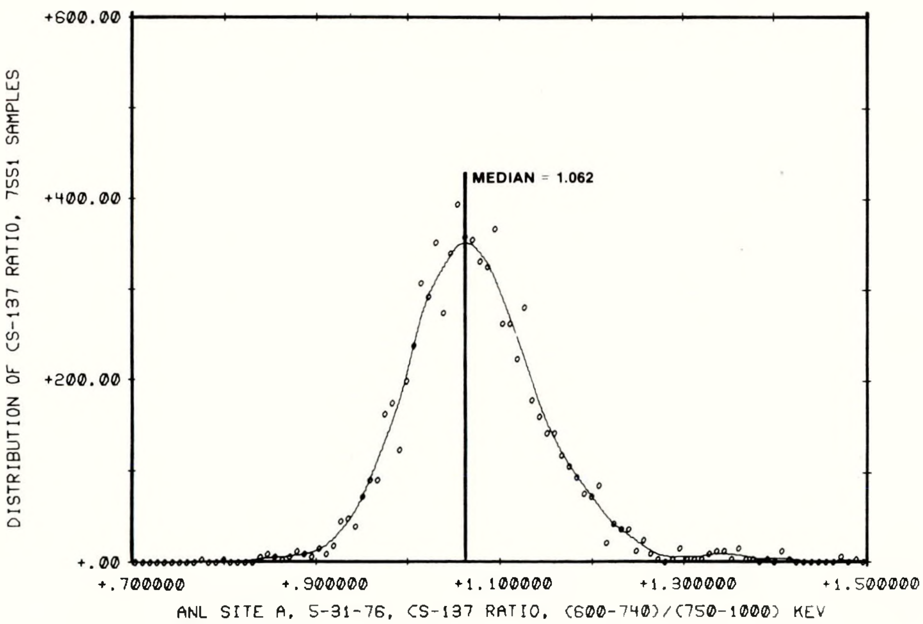


Figure 7. The ratio of two windows, containing the $^{137}Cs$ photopeak and background, was obtained from the survey data (7551 samples). The high skew of the pulse-height distribution indicates that some samples contain excessive $^{137}Cs$.

distributed, or uniformly distributed over the area where the data were taken. (Uniform distributions show a spread due to counting statistics.) However, the frequency distribution for the area in question was skewed with a high ratio tail, indicating the existence of pockets of $^{137}Cs$ concentrations significantly above the standard deviation in the data. Additional data from areas known to be lacking in $^{137}Cs$ are necessary in order to determine absolute concentrations. The aerially measured concentrations reported here will be those existing above the average over the survey area. The average concentration was suppressed by processing the data according to the following algorithm:

$$^{137}Cs = \Sigma(0.600, 0.740) - 1.062\ \Sigma(0.750, 1.000)$$

where $\Sigma(0.600, 0.740)$ is the sum of all counts in the 0.600 MeV to 0.740 MeV window. The 1.062 multiplier for the second window was determined from the median of the ratio distribution. Positive excursions in the algorithm (or ratio) above a preselected minimum are interpreted as excessive $^{137}Cs$. The results will be discussed in detail in Sec. 7.2. A 9-second, sliding interval average is applied to the final plotted results to reduce statistical anomalies.

It should be observed at this point that the detector system, at an elevation of 30 m, has a field-of-view much larger than instruments mounted 1 m above the soil surface. Figure 8 shows that this field is a circle whose diameter depends on the energy of the gamma ray measured. The greater the gamma ray energy the farther the gammas may travel before being attenuated by air.

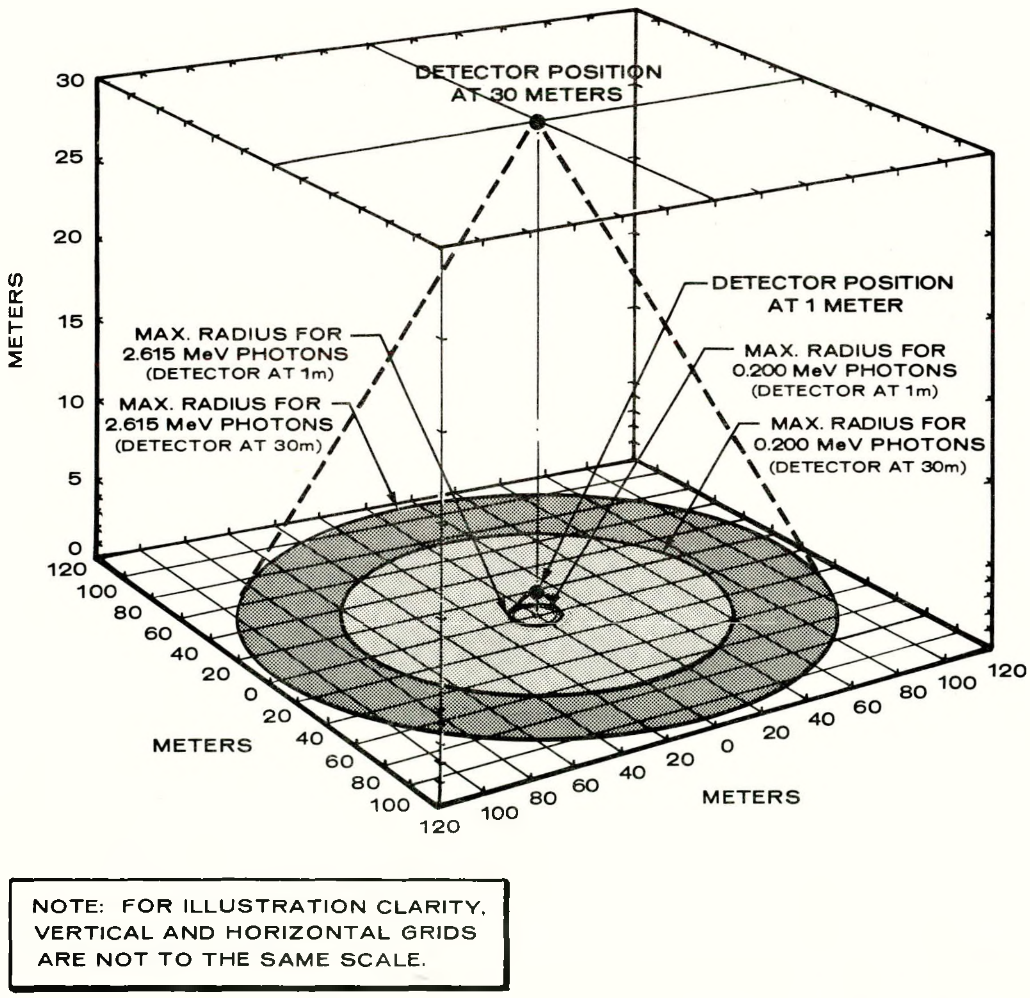


Figure 8. The detector field-of-view is a circle from which 90% of the detected photons emanate. The field varies with photon energy. At the 30 m survey altitude the detectors see an area 220 times larger than a hand-held detector system at 1 m.

For comparison, consider the detection of $^{208}Tl$ gamma rays at 1 m and 30 m. For all practical purposes, these were the most energetic ($E_\gamma$ = 2.615 MeV) gamma rays measured during this survey. Some thallium photons will collide with atoms of gas or suspended particulate matter between the ground and the detector. Then photons of degraded energy may be detected ("collided photons"). However, these have lost their identity as "thallium photons". Approximately 90% of the uncollided photons arriving at the detector (the "field-of-view") are emitted from a circle 7.93 m in radius when the detector is 1 m above ground. However, at the survey altitude of 30 m, this circle has a radius of 118.1 m. At 1 m the detector field-of-view encloses 198 $m^2$. At 30 m the field is 43,800 $m^2$, an area 220 times larger. At 61 m, the field-of-view has a radius of 183 m, an area of 152,200 $m^2$.

Most photons are from sources of lower energy; therefore, the field-of-view is smaller than these maximum values. However, the above numbers illustrate the following important facts:

A. The results of in situ measurements at 1 m, or from soil samples, must be averaged over a large area for comparison with aerial isopleths. Ion chamber measurements and soil samples are routinely collected along flight lines of AMS surveys. When properly averaged, the results are consistently within 20% of exposure rates determined from the air.[4][5]

B. An airborne detector may sense a source from some distance away. The degree to which a distant source affects the counting rate associated with a position directly beneath the aircraft depends, for contouring purposes, on the aircraft altitude, as well as activity and spatial extent of the source. For a gross count isopleth (Fig. 9) gamma rays of all energies between 50 keV and 3 MeV are collected. An intense, localized source of any energy generates both a direct, uncollided signal, and an indirect signal. The latter is caused by lower energy gammas scattered from the primary radiation. Both collided and uncollided gammas are counted. An intense source may affect a gross gamma isopleth 300-400 m away. This is called the "shine" effect.

On 27 May a total of 23 soil samples were gathered, 16 from Site A, 7 from Plot M. These were sent to the EG&G counting laboratory in Goleta, California. Samples 1 through 16 (from Site A) were oven dried and canned following standard procedures. Samples 17 through 23 (from Plot M) were freeze dried with a lyophilizer system in order to recover the extracted water to be analyzed for tritium concentrations. These were determined on a Beckman LS-100 liquid scintillation counter.

# 7.0 RESULTS

## 7.1 GROSS COUNT GAMMA ISOPLETH

Figure 9 is a gross count gamma radiation isopleth superposed on an aerial photograph of a portion of the Palos Hills Forest Preserve. The count rate has been converted to exposure rate of 1 m above ground in units of microroentgen per hour ($\mu$R/h). All background, except cosmic rays, have been removed. Hence, the isopleth shows gamma radiation due to terrestrial sources and an average (calculated) cosmic ray background of 4 $\mu$R/h.

The calibration flight over the Saganashkee Slough at the survey height of 30 m yielded an average gross count rate of 814 counts per second (cps). These counts originate from: (1) low level sources in the detectors, the electronic equipment, and the aircraft, (2) radon, thoron, and their daughter products, and (3) cosmic rays.

The background (814 cps) is subtracted from each gross count sum so that the result characterizes terrestrial sources only. Previous calibration work with this system indicates that 1230 cps (from terrestrial sources only) is equivalent to an exposure rate of 1 $\mu$R/h at an altitude of 1 m. Hence, the REDAC is programmed to plot count rate according to the following code:

Table 2. Gamma Gross Count Rate and Exposure Rate

| Letter Label | Count Rate (counts per second) | Exposure Rate ($\mu$R/h) |
|---|---|---|
| A | 0000 - 1230 | 4 - 5 |
| B | 1231 - 2460 | 5 - 6 |
| C | 2461 - 3690 | 6 - 7 |
| D | 3691 - 4920 | 7 - 8 |
| E | 4921 - 6150 | 8 - 9 |
| F | 6151 - 7380 | 9 - 10 |
| G | 7381 - 8610 | 10 - 11 |
| H | 8611 - 9840 | 11 - 12 |

The 4 $\mu$R/h cosmic ray contribution was added to the exposure rate calibration to make the isopleth easier to compare with other field measurements. This level was calculated from meteorological data and theoretical studies. From weather data at Chicago Midway Airport (at 1:50 pm CDT on 31 May 1976 the barometric pressure was 29.82 in, temperature 69° F, and dew point 61° F) one can calculate the air density during the survey as follows:

$$\rho = 1.19 \times 10^{-3} \text{ g/cm}^3$$

The total depth of the atmosphere has been estimated[6] at 1033 g/cm². Hence, the atmospheric depth at the survey site (elevation 221 m) is 26.3 g/cm² and the cosmic rays have penetrated to an atmospheric depth of 1006.7 g/cm².

The theoretical work of O'Brien and experimental confirmation by Liboff[7] allows one to compute the ionization and, hence, the exposure rate (E) due to cosmic rays:

$$E = \frac{2.32 \text{ ion pairs}}{\text{cm}^3 \text{ of NTP air}} \times \frac{1.73\ \mu\text{R/h}}{\text{ion pairs/cm}^3 \text{ of NTP air}} = 4.01\ \mu\text{R/h}$$

Although cosmic ray levels are known to vary, especially as a function of the 11 year solar activity cycle, the above result may be considered as a reasonable average value.

The result also agrees well with experimental measurements of the exposure rate at this latitude. Gustafson, et al,[8] measured $4.4 \pm 0.2\ \mu$R/h on a boat 3.2 km from shore on Lake Michigan. The effect was attributed primarily to mu-mesons, the most penetrating component of cosmic radiation.

The isopleth (Fig. 9) is dominated by the G contour (11 $\mu$R/h). Frequent and extensive excursions to the F and H contours are observed. These excursions appear to be normal, probably due to slight inhomogeneities in the distribution of naturally occurring isotopes. If one superposes the gross count (Fig. 9) and cesium (Fig. 10) isopleth maps, there is no strong correlation in the positions of the highest contour levels. Even though the burial site (Plot M) and part of Site A are covered by an H contour, these appear to have no special significance. Note that the contour is stepped in 1 $\mu$R/h intervals, and that H contours occur elsewhere in the isopleth in areas where radioisotopes were probably not used.

Several depressions in the radiation level are also apparent. Over small bodies of water or swampy areas the level drops to a C or D because the water attenuates the radiation arriving at the detectors. Over larger bodies of water, such as the Saganashkee Slough, the level drops to an A, indicating that the detectors see only background from cosmic rays, radon in the air, and aircraft background, the latter two of which have been subtracted from these data according to the aforementioned algorithm. Over the Calumet Sag Channel the level drops only to a B because it is extremely narrow (approximately 75 m). Even when the helicopter is directly over the Channel, the detector field-of-view overlaps both banks. Figure 8 indicates that the radius of the field-of-view is nearly 120 m for the photons of highest energy.

Radiation levels measured here are typical of background levels in the Midwest.[9] Hence, the gross count map itself does not suggest strong contamination within the survey boundaries. The gamma spectra and the cesium isopleth, however, do provide evidence of low level contamination.

### 7.2 $^{137}$Cs ISOPLETH MAP

The values of the algorithm defined in Sec. 6.0 were smoothed over approximately nine seconds to reduce statistical fluctuations and increase sensitivity to $^{137}$Cs. (It should be mentioned that smoothing operations decrease spatial resolution along the flight path.) These averaged values were then assigned the following codes and plotted as a function of position:

Table 3. $^{137}$Cs Count Rates

| Letter Label | Gamma Count Rate Above Average Over Site (cps at 30 m altitude) |
|---|---|
| A | 1 - 22 |
| B | 23 - 27 |
| C | 28 - 33 |
| D | 34 - 39 |
| E | 40 - 47 |
| F | 48 - 56 |

This algorithm effectively isolates the 0.662 MeV photopeak of $^{137}$Cs above the average over the survey area and subtracts the background due to cosmic rays, radon gas, and sources within the aircraft or detector systems.

The cesium isopleth map (Fig. 10) shows some correlation with Site A, but perhaps not with Plot M. An F contour covers Site A and extends 180 m east and 180 m west of the perimeter road. These results corroborate soil sample data (Sec. 7.4) from Site A.

A D contour is centered 200 m northwest of Plot M. This activity is not obviously correlated with Plot M and, unfortunately, no soil samples were taken from the area under this contour.

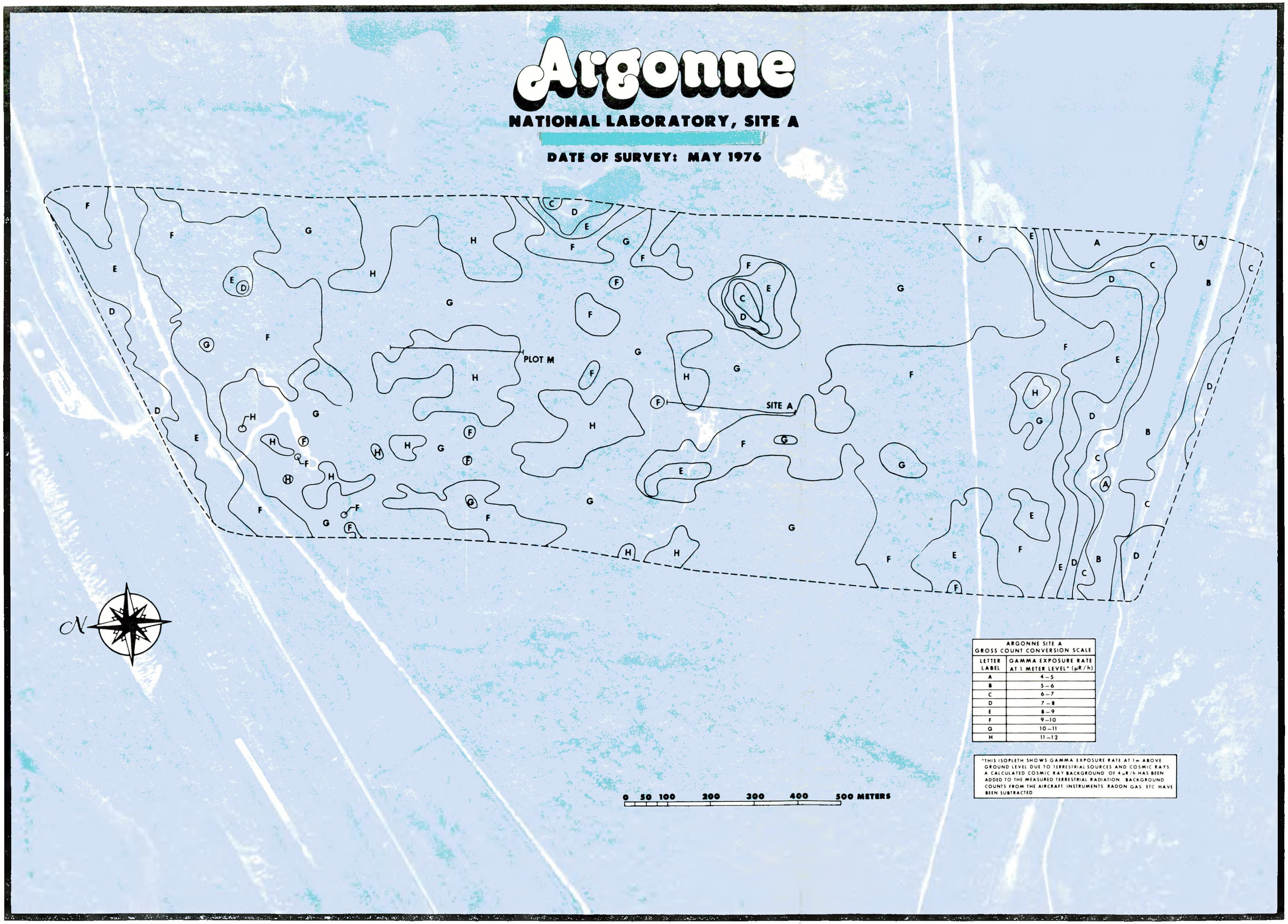


| ARGONNE SITE A GROSS COUNT CONVERSION SCALE | |
|---|---|
| LETTER LABEL | GAMMA EXPOSURE RATE AT 1 METER LEVEL* (μR/h) |
| A | 4–5 |
| B | 5–6 |
| C | 6–7 |
| D | 7–8 |
| E | 8–9 |
| F | 9–10 |
| G | 10–11 |
| H | 11–12 |

Figure 9. The gamma gross count isopleth shows exposure rate due to gamma rays with energies between 50 keV and 3 MeV. Lines were flown at a 30 m altitude with 30 m spacing. The results are normalized to 1 m above ground.

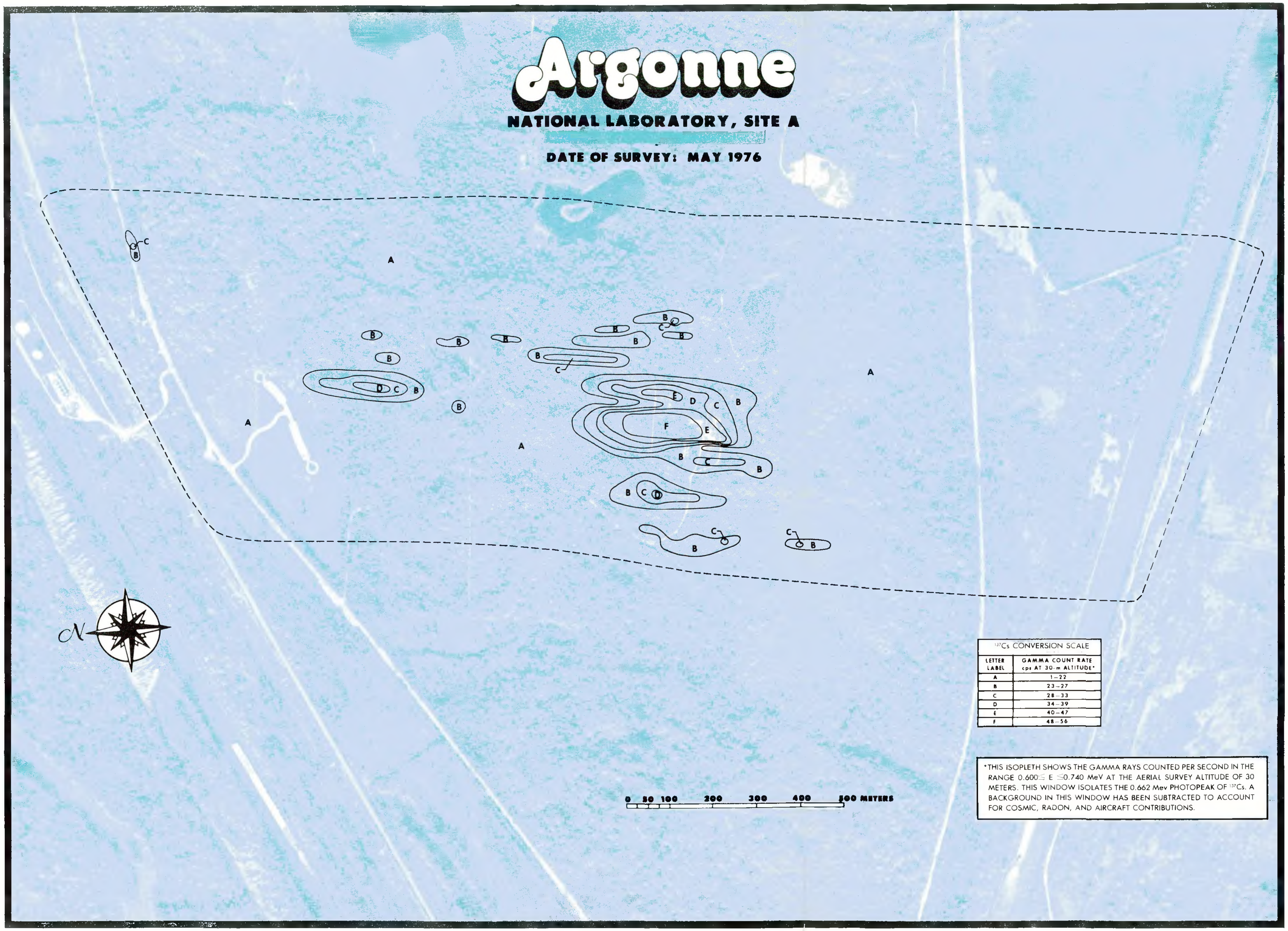


$^{137}$Cs CONVERSION SCALE

| LETTER LABEL | GAMMA COUNT RATE cps AT 30-m ALTITUDE* |
|---|---|
| A | 1–22 |
| B | 23–27 |
| C | 28–33 |
| D | 34–39 |
| E | 40–47 |
| F | 48–56 |

Figure 10. A computer algorithm was devised to extract evidence of excessive $^{137}$Cs in the aerial spectra. Concentrations far removed from Site A operations may be due to worldwide $^{137}$Cs which has drained to, and accumulated at, low spots in the area.

It would seem unlikely that worldwide fallout of $^{137}Cs$ would occur in such highly localized concentrations. Soil sample results (Sec. 7.4) indicate average $^{137}Cs$ concentrations three times higher than typical locations in the Midwest.

Therefore, one may tentatively conclude that the observed cesium may be attributed to research activity conducted many years ago at Site A.

To estimate soil concentration of the $^{137}Cs$, one needs more information. In particular, one must know soil composition and soil moisture. More importantly, the $^{137}Cs$ concentration must be measured as a function of soil depth. Since this was not done as part of the present work, we can construct the following conversion chart by making some reasonable estimates:

Table 4. $^{137}Cs$ Soil Concentrations

| $\alpha/\rho$ (cm²/g) | $1/\alpha$ (cm) | Conversion Factor ($\mu$Ci/m² per count/sec) |
|---|---|---|
| 6.25 | 0.1 | $8.64 \times 10^{-4}$ |
| 0.625 | 1.0 | $1.06 \times 10^{-3}$ |
| 0.312 | 2.0 | $1.26 \times 10^{-3}$ |
| 0.206 | 3.0 | $1.46 \times 10^{-3}$ |
| 0.0625 | 10.0 | $2.76 \times 10^{-3}$ |

where: $\alpha/\rho$ is the depth distribution (cm²/g)

$\rho$ is the soil bulk density (g/cm³)

$1/\alpha$ is the relaxation length of the assumed exponentially-distributed source activity with depth (cm)

To make the above calculations, we have assumed that the aircraft altitude is 30.5 m, the gamma mean free path in air is $\lambda_a = 113$ m, and that the mass attenuation coefficient for the soil is $\mu_s/\rho = 0.0788$ cm²/g. We further assume a standard soil composition with 10% moisture content.[10] Hence, if the soil around Site A shows a relaxation depth of 2 cm, the maximum concentration there would be $7.1 \times 10^{-4}$ $\mu$Ci/m²; for 3 cm, the concentration would be $8.2 \times 10^{-4}$ $\mu$Ci/m².

## 7.3 GAMMA SPECTRA FROM AERIAL SURVEY

By analyzing gamma ray intensity vs. energy spectra, the analyst can identify the major contributors in a mixed gamma ray source. It should be noted that the poor resolution of NaI(Tl) detectors (approximately 8-10%), coupled with the large number of photopeaks in the uranium and thorium decay series, means that closely spaced peaks may merge inseparably. (The FWHM [full width at half of the maximum photopeak height] is commonly used as a measure of detector resolution, and for the thallium photopeak at 2.615 MeV this width is frequently 200-260 keV.) Where the strong contributors have been introduced by human activity at the survey site, such radioisotopes are best identified by a background subtraction.

Spectra from aerial data over Site A and Plot M show appreciable differences from the background spectra. Figure 11 shows all of the data accumulated during line 27, which is 275 m west of the center of Site A. The actual flight path for line 27 is shown as line segment 27 in Fig. 3. The spectrum shows 747,447 photons counted during 1.75 minutes. (A total of 35 records are displayed, each representing 3 seconds of clock time.) The live time (1.695 min) indicates a dead time loss of 3.1%, which is acceptable. Dead time losses were compensated for when the gross count isopleth (Fig. 9) was generated. Note that the spectrum showing least detail is plotted on a scale of $10^5$ counts full scale. The spectrum is enlarged three times (x 10, x 100, x 1000) to display details at low count rates.

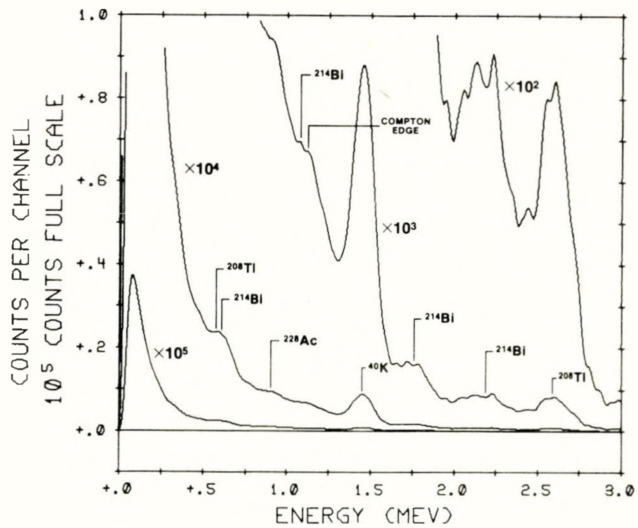


Figure 11. The above gamma counts were accumulated during the 105 second interval required to fly line 27, which is far enough from Site A and Plot M to be considered background. Dead time is 3.1%

The following nuclides are the major contributors to the spectrum in Fig. 11:

Table 5. Nuclides in the Site A Background

| Energy (MeV) | Isotope |
|---|---|
| 0.583 | $^{208}$Tl |
| 0.609 | $^{214}$Bi |
| 0.911 | $^{228}$Ac |
| 1.120 | $^{214}$Bi |
| 1.461 | $^{40}$K |
| 1.764 | $^{214}$Bi |
| 2.204 | $^{214}$Bi |
| 2.615 | $^{208}$Tl |

There are, of course, many other photopeaks of the preceding isotopes, and other naturally occurring radioisotopes, which contribute to the spectrum. Their photopeaks are not apparent because they are less intense than those shown or they occur at energies dominated by other photopeaks.

Apparent photopeaks in the spectrum at 1000, and especially at 100, counts full scale may be real or the result of statistical fluctuations in the low count rates encountered at high energies. Structural "detail" in the 2.615 MeV $^{208}$Tl photopeak provides the clue to this problem. The resolution of this peak is 260 keV (FWHM), about 10%. Weak $^{228}$Ac peaks at 1.4958-, 1.5015-, 1.5569-, 1.5802-, 1.5879-, 1.6247-, 1.6304-, and 1.6380-MeV are probably hidden in the high energy tail of the $^{40}$K photopeak. Similarly, the many weak photopeaks of $^{214}$Bi which occur between those shown are considerably weaker and readily obscured.

Note the apparent photopeak near the 1.120 MeV photopeak of $^{214}$Bi. This appears on many spectra drawn from this survey area. It is apparently the Compton edge for $^{40}$K photons, which occurs at approximately 1.13 MeV. The $^{40}$K photopeak is relatively strong in this area in comparison to $^{214}$Bi. Hence, we might expect the Compton edge to be more prominent.

Figure 12 is a spectrum recorded directly over Site A. The helicopter path is noted on Fig. 3. Since this spectrum shows only nine seconds of data, the results are statistically less reliable. Nevertheless, the same peaks show up. In addition, one notes that the unresolved 0.583 MeV ($^{208}$Tl) plus 0.609 MeV ($^{214}$Bi) peak is broader and taller. Since the cesium contribution is weak, it does not dominate the spectrum.

Figure 13 is a spectrum recorded over Plot M which is also nine seconds in duration. The peaks at 1.12 and 1.13 MeV have apparently merged into one larger peak. However, little significance can be attached to this because of counting statistics. It also appears that

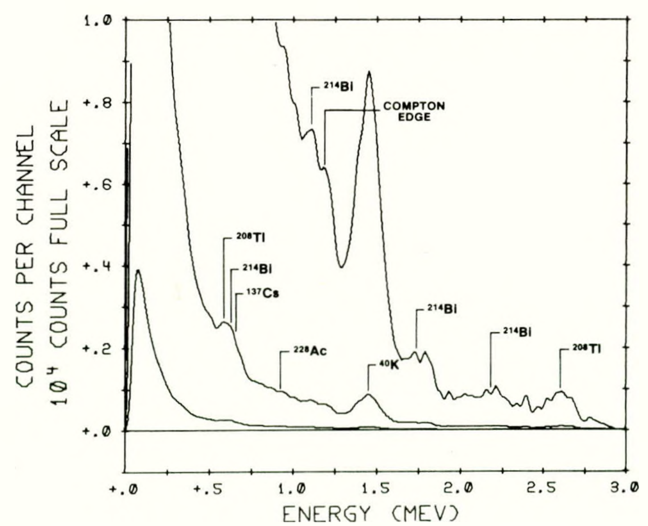


Figure 12. This 9 second spectrum was accumulated as the H-500 flew over Site A on line 14. The line segment is marked on Fig. 3.

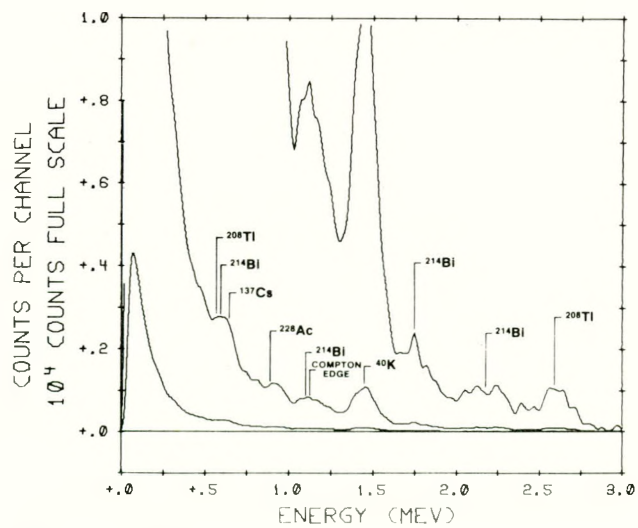


Figure 13. This 9 second spectrum was accumulated as the H-500 flew over Plot M on line 17. The line segment is marked in Fig. 3.

the 0.860 MeV peak of $^{208}Tl$ is visible here. Note that the 0.583 + 0.609 MeV peak is again broadened, but not dominated, by an apparent contribution from $^{137}Cs$. From these spectra one can conclude that the contamination levels are lower (over Site A and Plot M) than can be readily detected with a single aerial pass using our detector system.

However, with the assistance of the computer, one can accumulate data over all portions of the survey area which appear to contain abnormal cesium concentrations. All data records (inclusive from lines 12 through 22) which contributed B or higher levels to the cesium algorithm (Fig. 10) were summed. All data from these 11 lines were treated as background and subtracted from the "cesium loaded" spectra. The net spectrum (Fig. 14) shows a strong contribution at the Cs photopeak energy, 0.662 MeV. Even in this case the peak area is distorted, indicating a relatively low level of cesium contamination.

### 7.4 SOIL ANALYSIS

The results of the gamma ray spectroscopy and other data are summarized in Table 6, which lists the dry sample mass, the moisture content, and the total gamma count above the threshold. Since none of the dry samples were large enough to fill the whole sample counting volume, quantitative information about the isotopes present could not be readily calculated. Therefore, Table 6 lists the photopeak intensity of the $^{137}Cs$ line (662 keV) relative to the $^{40}K$ line (1460 keV). Similar ratios are calculated for the 583 keV ($^{208}Tl$) line of the thorium decay chain, and the 609 keV ($^{214}Bi$) line

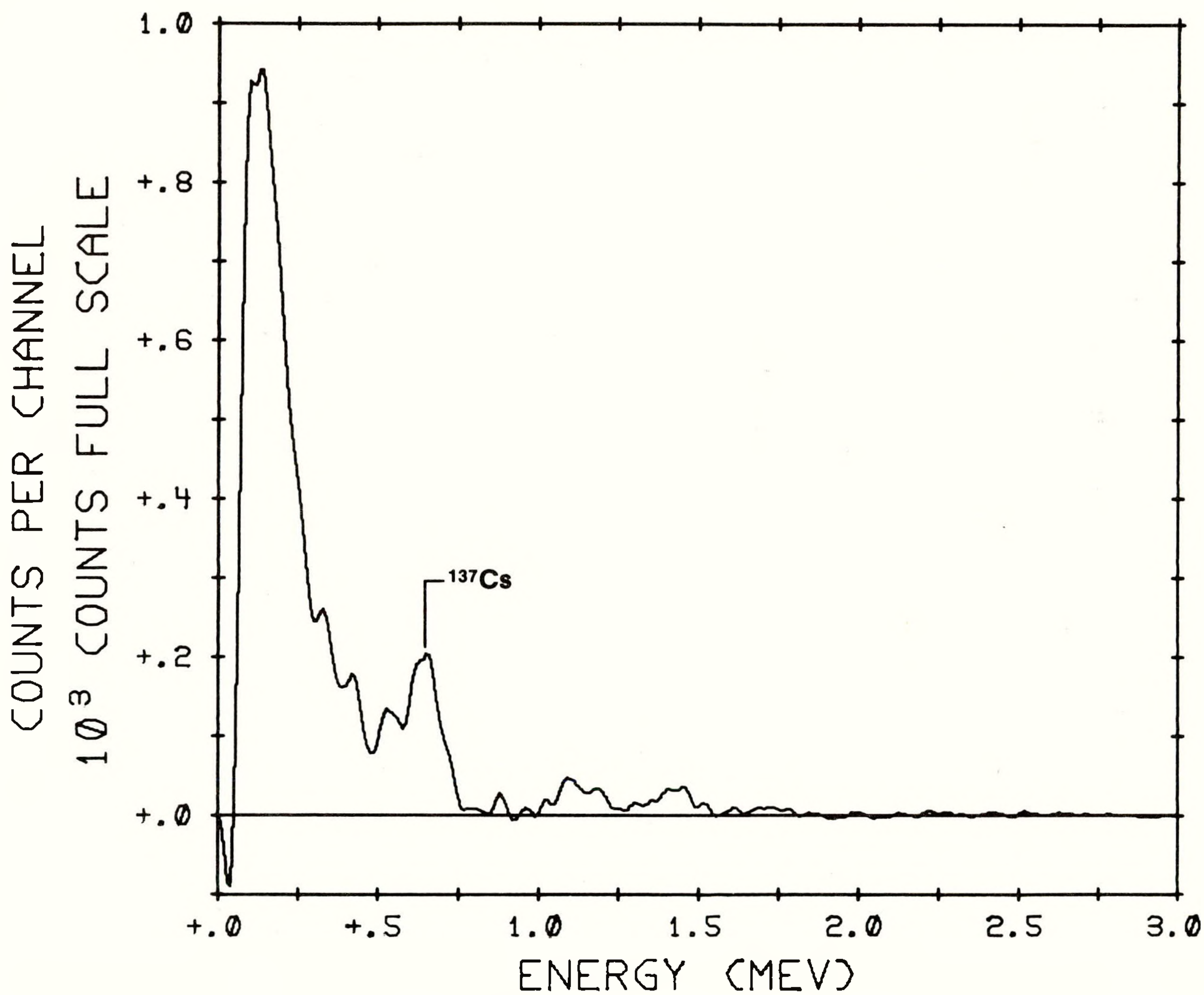


Figure 14. All gamma spectra from lines 12-22 were examined for above normal intensity "hot spots" in the cesium window (600-740 keV). For eight such regions, all counts were summed. All data from lines 12-22 were then subtracted. The net spectrum shows an enhanced $^{137}Cs$ photopeak at 662 KeV.

of the $^{238}U$ decay chain. For comparison the last row in the table shows the average value of these ratios calculated from the data of all the soil samples collected at Site No. 1 of the Duane Arnold Power Reactor survey in Palo, Iowa.[11]

The average value of the $^{137}Cs/^{40}K$ ratio at Argonne is 0.53 ± 0.35, more than three times the value measured at Duane Arnold. Although this increase could be caused by lower concentrations of $^{40}K$ at Argonne than at Duane Arnold, a factor of three is not expected. It is even more instructive to consider the large standard deviation associated with the ratio values for Argonne data (± 66%) relative to that associated with the Duane Arnold data (± 29%). Since the Argonne soil sample data were taken over areas small enough so that the $^{40}K$ concentrations should

Table 6. Argonne Soil Sample Results.

| Sample Number | Mass (g) | Total Counts | Moisture % | Cs/K $\left(\frac{662}{1460}\right)$ | Th/K $\left(\frac{583}{1460}\right)$ | U/K $\left(\frac{609}{1460}\right)$ |
|---|---|---|---|---|---|---|
| 1 | 20.5 | 99,872 | 2.9 | 1.59 | 0.16 | 0.17 |
| 2 | 17.8 | 86,759 | 22.5 | 0.61 | 0.15 | 0.18 |
| 3 | 50.8 | 112,626 | 33.1 | 0.67 | 0.13 | 0.18 |
| 4 | 50.7 | 94,122 | 7.7 | 0.98 | 0.16 | 0.18 |
| 5 | 62.1 | 145,259 | 24.3 | 0.40 | 0.14 | 0.37 |
| 6 | 69.2 | 113,156 | 51.0 | 0.27 | 0.12 | 0.21 |
| 7 | 35.6 | 96,394 | 53.9 | 0.48 | 0.13 | 0.21 |
| 8 | 134.7 | 195,712 | 35.2 | 0.67 | 0.14 | 0.37 |
| 9 | 47.0 | 128,986 | 3.8 | 0.80 | 0.16 | 0.48 |
| 10 | 38.7 | 103,752 | 1.3 | 0.73 | 0.13 | 0.26 |
| 11 | 26.7 | 102,732 | 13.1 | 0.12 | 0.09 | 0.21 |
| 12 | 29.1 | 97,776 | 39.5 | 0.51 | 0.12 | 0.21 |
| 13 | 38.3 | 135,114 | 1.0 | 1.02 | 0.14 | 0.37 |
| 14 | 70.3 | 163,984 | 1.2 | 0.15 | 0.13 | 0.31 |
| 15 | 66.9 | 133,868 | 0.8 | 0.64 | 0.17 | 0.38 |
| 16 | 28.1 | 100,515 | -0- | 0.24 | 0.13 | 0.20 |
| 17 | 18.5 | 99,393 | 4.2 | 0.31 | 0.12 | 0.16 |
| 18 | 34.6 | 98,324 | 9.0 | -0- | 0.07 | 0.21 |
| 19 | 53.4 | 105,466 | 4.0 | 0.39 | 0.14 | 0.27 |
| 20 | 12.5 | 82,971 | 9.5 | 0.61 | 0.15 | 0.14 |
| 21 | 8.0 | 80,932 | 3.7 | 0.49 | 0.18 | 0.13 |
| 22 | 34.9 | 119,139 | 1.0 | 0.42 | 0.12 | 0.23 |
| 23 | 29.5 | 98,752 | 15.9 | 0.11 | 0.09 | 0.23 |
| Duane Arnold Site No. 1 | | | | 0.17 ± 0.05 | 0.19 ± 0.05 | 0.27 ± 0.04 |

show small variations, it must be assumed that the $^{137}$Cs concentrations show large variations over dimensions comparable to the separation between the points where soil samples were taken. These data, on a microscopic scale, support the aerial data, on a macroscopic scale.

Figure 15 shows a typical gamma ray spectrum of a Site A soil sample measured with the Ge(Li) detector. The measured $^{137}$Cs/$^{40}$K ratio of 0.15 is typical of midwestern sites. Sample 8 (Fig. 16) had the only spectrum with distinct $^{60}$Co lines (1.17 and 1.33 MeV). Sample 1 (Fig. 17) has the strongest indication of $^{137}$Cs, as well as two unidentified gamma lines at 2.274 and 2.457 MeV. Both of the uranium daughters $^{214}$Bi and $^{210}$Tl have lines in these areas, but the energy errors are greater than normal. Other isotopes have minor lines at these energies, but their confirming gamma lines are missing from the spectrum. For example, $^{140}$La has a 2.4654 MeV gamma but the confirming and more intense line at 1.596 MeV is missing.

### 7.5 SOIL MOISTURE ANALYSIS

Seven soil samples were freeze dried and the extracted water analyzed for $^{3}$H content using the Beckman LS-100 liquid scintillation counter system. Sample 17 yielded insufficient water for analysis. Samples 20, 21, and 22 contained too little water to accurately measure the water sample volume, so the resulting $^{3}$H concentration values are approximate due to the uncertainty in the volume. The remaining three samples contained enough water to mix a standard counting solution (2 ml $H_2O$ in 10 ml scintillation cocktail). The results are as follows:

Table 7. Plot M Soil Moisture Analysis

| Sample Number | Gross Sample Mass(g) | Concentration of $^{3}$H in Extracted Water (pCi/ml) |
|---|---|---|
| 17 | 18.5 | Insufficient water for analysis |
| 18 | 34.6 | $1.15 \times 10^4$ |
| 19 | 53.4 | $3.11 \times 10^3$ |
| 20 | 12.5 | Approx. $5.3 \times 10^1$ |
| 21 | 8.0 | Approx. $1.86 \times 10^2$ |
| 22 | 34.9 | Approx. $1.77 \times 10^2$ |
| 23 | 29.5 | $1.31 \times 10^2$ |

For comparison, a counting sample containing 2 ml of Goleta, California, tap water was analyzed: the $^{3}$H concentration was 5.4 pCi/ml. Sample 18 shows a tritium concentration 2000 times greater.

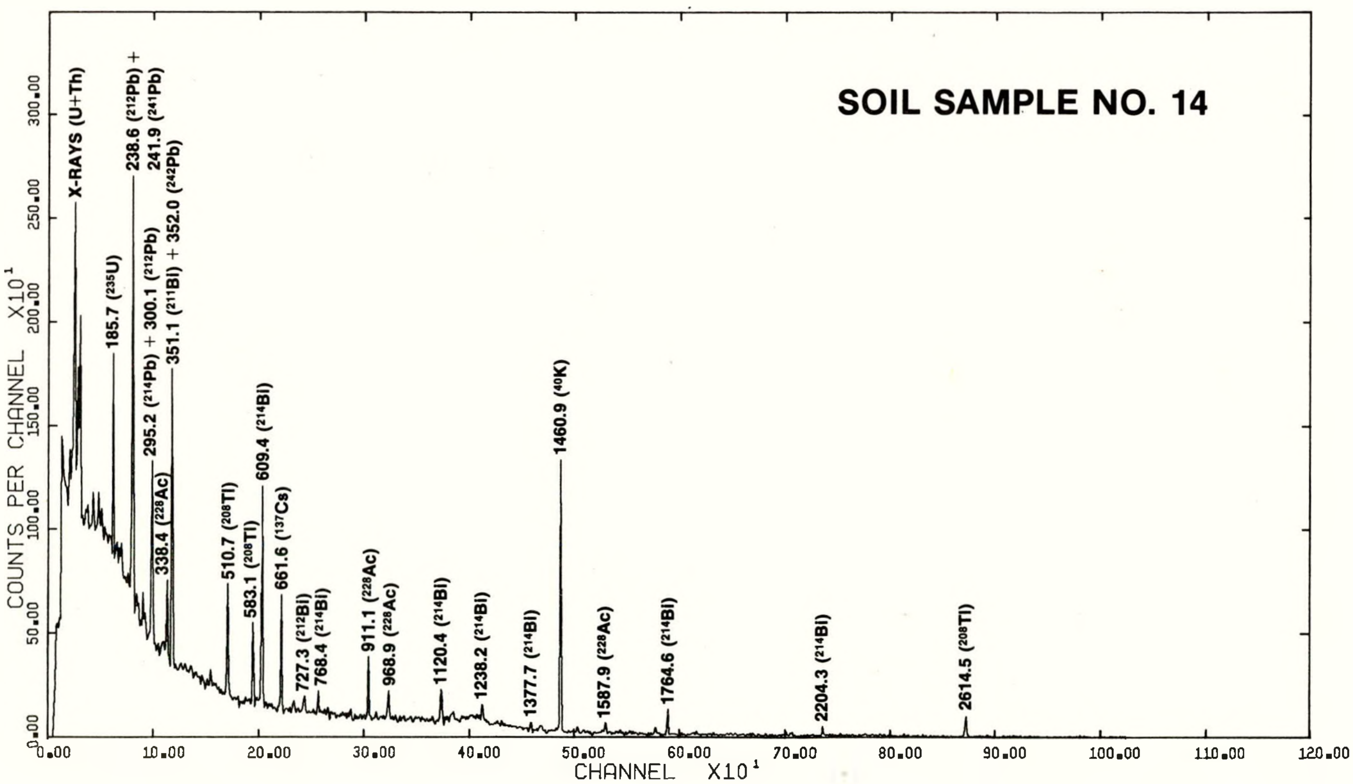


Figure 15. Soil sample 14 (sample location shown in Fig. 3) was counted on a Ge(Li) detector with an absolute efficiency of 8%, analyzed on a 1024 channel analyzer. Most of the photopeaks are naturally occurring daughters of uranium and thorium. However, slight contamination by $^{137}$Cs (661.6 keV) is apparent in this sample. Energies are expressed in kiloelectronvolts (keV).

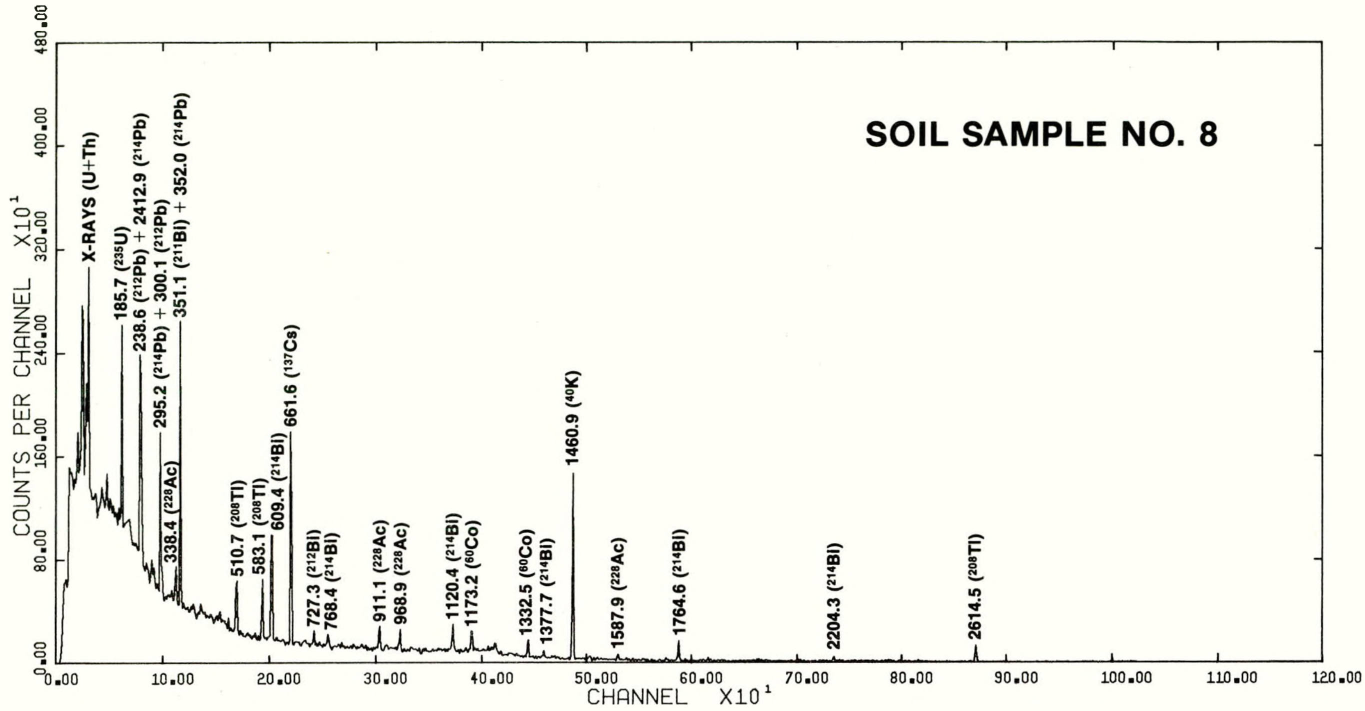


Figure 16. Soil sample 8 was counted and analyzed with the same equipment as for Fig. 15. Sample location is shown in Fig. 3. Both $^{137}Cs$ (661.6 keV) and $^{60}Co$ (1173.2 and 1332.5 keV) contamination appear here. Energies are expressed in keV.

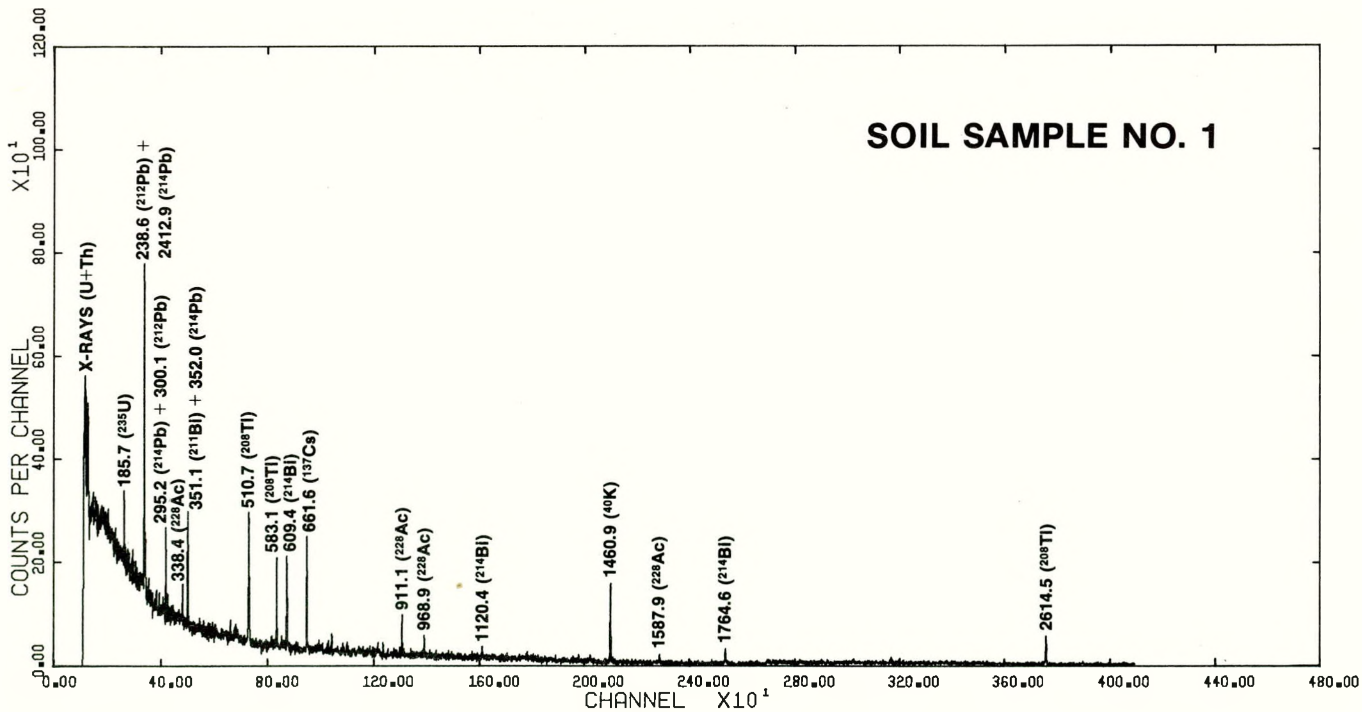


Figure 17. Soil sample 1 was counted on a Ge(Li) detector with an absolute efficiency of 15%, analyzed with a 4096 channel analyzer. Sample location is shown in Fig. 3. This sample shows relatively strong $^{137}Cs$ contamination. Energies are expressed in keV.

## 8.0 CONCLUSION

The aerial survey shows measurable concentrations of $^{137}Cs$ over Site A and near Plot M, which can probably be attributed to reactor operations. Soil samples from these areas show $^{137}Cs$, $^{60}Co$, and traces of other contaminants. Water extracted from Plot M soil samples also showed tritium, a $\beta$-emitter which cannot be detected from the aircraft.

## REFERENCES

1. Boyns, P. K., "The Aerial Radiological Measuring System (ARMS) Systems, Procedures and Sensitivity (1976)," Report No. EGG-1183-1691, EG&G, Las Vegas, NV, July 1976.

2. Jobst, J. E., "An Aerial Radiological Survey of the Idaho National Engineering Laboratory (Idaho Falls, Idaho), Date of Survey: 15 August to 11 September 1974," Report No. EGG-1183-1681, EG&G, Las Vegas, NV, November 1976.

3. Quam, W., Houk, J., and Mohr, R., "Low Background Ge(Li) Detector with Anticoincidence NaI Annulus (Revised)," Report No. EGG-1183-2326 (Rev), EG&G, Goleta, CA, February 1976.

4. Franks, L. A., EG&G, Goleta, CA, private communication.

5. Mohr, R., Fritzsche, A., and Franks, L., "Ground Survey Procedures," Report No. EGG-1183-2339, EG&G, Goleta, CA, January 1976.

6. O'Brien, K., "The Cosmic Ray Field at Ground Level," *The Natural Radiation Environment II,* Report No. CONF-720805-P1, August 1972, p. 15.

7. Liboff, A. R., "Cosmic Ray Ionization in the Lower Atmosphere," *The Natural Radiation Environment II,* Report No. CONF-720805-P1, August 1972, p. 55.

8. Gustafson, P., Kastner, J., and Luetzelschwab, J., "Environmental Radiation: Measurement of Dose Rates," Science, July 1964, 145:44-47.

9. Jobst, J. E., "An Aerial Radiological Survey of the Weldon Spring Checmical Plant (St. Charles, Missouri), Date of Survey: 11-14 May 1976," Report No. EGG-1183-1700, EG&G, Las Vegas, NV, December 1976.

10. Beck, H. L., Decampo, J., and Gogolak, C., "In Situ Ge(Li) and NaI(Tl) Gamma-Ray Spectroscopy," Report No. HASL-258, U.S.A.E.C., New York, NY, September 1972.

11. Boyns, P. K., "Aerial Radiological Survey of the Duane Arnold Energy Center (Palo, Iowa), Date of Survey: June 1976," Report No. EGG-1183-1699, EG&G, Las Vegas, NV, February 1977.

# DISTRIBUTION

**DOE/DOES**

L. J. Deal (15)

**DOE/DMA**

R. E. Lounsbury (1)

**DOE/NV**

D. G. Jackson (3)
J. A. Koch (1)
R. B. Loux (1)
R. J. Peterson (5)
R. B. Purcell (2)
Resident DOE, EMO (1)

**DOE/TIC**

T. B. Abernathy (2)

**H&N**

W. E. Anderson (1)

**REECo**

H. E. LaPlant (1)

**ARGONNE**

J. Sedlet (10)

**EG&G**

R. H. Beers, WAMD (2)
H. M. Borella, SBO (2)
J. F. Doyle, LVO (1)
L. A. Franks, SBO (1)
J. E. Jobst, LVO (1)
H. A. Lamonds, SBO (1)
R. L. Lynn, SBO (1)
R. A. Mohr, SBO (1)
L. G. Sasso, LVO (1)
G. P. Stobie, LVO (1)
E. J. Story, LVO (1)
T. P. Stuart, LVO (1)
W. J. Tipton, LVO (1)

**LIBRARIES**

AMO (50)
Las Vegas (1)
Santa Barbara (2)